Correlation between Peak SAR and Maximum Temperature Increase Due to Dipole Antenna above 3GHz

Akimasa Hirata [1], Osamu Fujiwara [1], and Toshiyuki Shiozawa [2]

[1] *Department of Computer Science and Engineering, Nagoya Institute of Technology*
Gokiso-cho, Showa-ku, Nagoya 466-8555, Japan, ahirata@nitech.ac.jp, fujiwara@elcom.nitech.ac.jp
[1] *Department of Electronics and Information Engineering, Chubu University*
Kasugai 487-8501, Japan, shiozawa@isc.chubu.ac.jp

Abstract

Peak SAR (specific absorption rate) averaged over any 1 or 10g of body tissue is used as a measure for the protection of RF near-field exposure in safety guidelines. However, physiological effects and damage to humans by EM wave exposures are induced by temperature increases. In our previous work, we discussed the correlation maximum temperature increases in the head with peak spatial-average SAR over the frequency bands from 900 MHz- 2.5 GHz. In this study, we extend the discussion to the frequency band from 1 GHz to 10 GHz, which covers the fourth generation mobile cellular system, wireless LAN, and so forth. The motivation of this study is that the SAR is more localized around the antenna due to the reduction of physical size of antenna, and thus further discussion is required for correlating SAR and temperature elevations. In particular, 3-D Green function for bio-heat equation is introduced in order to give insight for heat diffusion in human tissue.

1. INTRODUCTION

International and domestic organizations have established safety guidelines for human protection against EM wave exposure. For RF near field exposure, these guidelines are based on peak spatial SAR (specific absorption rate) averaged any 1 or 10g of body tissue. Incidentaly, note that a different averaging scheme is used for each guideline. However, physiological effects and damage to humans by EM wave exposures are induced by temperature increases. A temperature increase of 4.5 $^{\circ}$C in the brain has been noted to be an allowable limit which does not lead to any physiological damage (for exposures of more than 30 minutes). Additionally, the threshold temperature for pricking pain in skin is 45 $^{\circ}$C, corresponding to the temperature increase of 10-15 $^{\circ}$C. In view of these circumstances, the temperature increase in the anatomically-based human head model due to handset antennas has been calculated in several works (e.g., [1]-[3]). Particularly, we revealed that maximum temperature increases in the head and brain are reasonably proportional to peak SARs in these regions [4]. The frequency band considered was from 900 MHz to 2.5 GHz, which are assigned to cellular telephones.

The fourth generation mobile cellular system will be deployed around the year 2010. The most promising frequency band for this system is 4 to 5 GHz band. The frequency band assigned for wireless LAN is at 5.8 GHz. It is instructive to investigate correlation between maximum temperature increase and peak spatial-average SAR in the frequency bands which cover such emerging wireless technologies. In the frequency band above 3 GHz, safety guidelines have not yet been harmonized. Then, our attention is extended to the frequency band from 1 to 10 GHz. Firstly, by using a one-dimensional model, we discuss uncertainty of tissue composition [5] on this correlation. Next, three-dimensional cubic model is used to investigate the effect of antenna dimension on the correlation. Furthermore, some computational examples are presented for confirming the results using simplified human head models. Note that the SAR averaging schemes prescribed in the ICNIRP guideline [6] and IEEE standard [7] are considered in this paper.

2. MODELS AND METHODS

Three scenarios are treated in this study. Firstly, a seven-layered one-dimensional model [5] is considered to discuss the uncertainties caused by tissue inhomogeneity. Then, a three-dimensional cubic model is considered for investigating the effect of finite dimension of an antenna. Furthermore, an anatomically-based head model developed at Nagoya Institute of Technology [8] is used in order to confirm the finding obtained using the simplified human head models.

For calculating the temperature elevation due to microwave energy, first, the SAR in the model is calculated with the FDTD method. Then, the temperature rise is calculated by substituting SAR values obtained into the bio-heat equation. The thermal parameters in [2] are used in this study.

A. FDTD method

1-D and 3-D FDTD methods were used for calculating SAR in human tissues. In the 1-D case, a plane wave was considered as a source, while dipole antenna was considered

in the 3-D cases. For truncating computational region in the FDTD method, 12-layered PML was applied in all cases.

B. Temperature Calculation

The temperature in the human body is calculated by solving the bioheat equation. The SAR calculated by the FDTD method is used as the heat source. The bioheat equation [9], which takes into account the heat exchange mechanisms such as heat conduction, blood flow, and EM heating, is represented by the following equation:

$$C(r)\rho(r)\frac{\partial T(r,t)}{\partial t} = \nabla \cdot (K(r)\nabla T(r,t)) + \rho(r)SAR(r) + A(r,t)$$
$$- B(r,t)(T(r,t) - T_B(t)) \qquad (1)$$

where T is the temperature of the tissue, T_b the temperature of the blood, K the thermal conductivity of the tissue, C the specific heat of the tissue, Q metabolic heat generation, and B the term associated with blood flow.

The temperature increase due to the antennas is assumed to be so small that it cannot activate the thermoregulatory response: the increase of local blood flow, the activation of sweating mechanism, and so forth. Thus, this effect is neglected in our discussion. The boundary condition for Eq. (1) is given by

$$- K(r)\frac{\partial T(r,t)}{\partial n} = H \cdot (T_s(r,t) - T_e(t)) + SW(r,T_s(r,t)) \qquad (2)$$

where H, Ts, and Te denote, respectively, the heat transfer coefficient, the surface temperature of the tissue, and the temperature of the air. The finite-difference expressions for Eqs. (1) and (2) are given in [1, 2].

C. Green's Function of Bioheat Equation

The temperature increase in the human model due to EM waves gets saturated or becomes maximal at the thermally steady state. For this reason, the temperature increase at the thermally steady state is considered in this paper, corresponding to the worst case estimation. Eqs. (1) and (2) are reduced to the following equations at the thermally steady state:

$$C(r)\rho(r)\frac{\partial \delta T(r,t)}{\partial t} = \nabla \cdot (K(r)\nabla \delta T(r,t)) + \rho(r)SAR(r)$$
$$- B(r,t)\delta T(r,t) \qquad (3)$$

$$\left(H + K(r)\frac{\partial}{\partial n}\right)\delta T(r) = 0 \qquad (4)$$

where $\delta T(r)$ is the temperature increase of tissue. Eq. (3) is a linear differential equation subject to the boundary condition (2). The equation (3) with the boundary condition (4) means that the temperature increase and SAR distributions do not correspond to each other. However, the temperature increase is linear in terms of the output power of the antenna, or the SAR amplitude at the thermally steady state. Note that it takes 30 minutes or more before the temperature increase gets saturated. It is also noteworthy that Q and C do not affect the temperature increase at the thermally steady state. Let us consider this problem on the basis of a Green's function. Note that the Green's function corresponding to (3) was firstly

applied to the bioheat equation in [10, 11]. Green's function satisfies the following equations:

$$L(r)G(r;r_i) = -\delta(r - r_i) \qquad (5)$$
$$L(r) = \nabla \cdot (K(r)\nabla) - B(r) \qquad (6)$$

where $G(r;r_i)$ is a Green's function associated with the differential operator L. The Green's function is dependent on the blood flow and heat conductivity, together with the heat transfer coefficient corresponding to air temperature (See Eq. (2)).

The temperature increase at a particular position is given in the discretized form as:

$$\delta T(r) = \sum_i \rho(r_i)SAR(r_i)G(r;r_i) \qquad (7)$$

The Green's function for the bioheat equation will be evaluated later.

3. COMPUTAIONAL RESULTS

A. Green's Function of Bioheat Equation in Human Tissues

This section presents Green's functions in order to give some insight into temperature increase in human tissues due to the
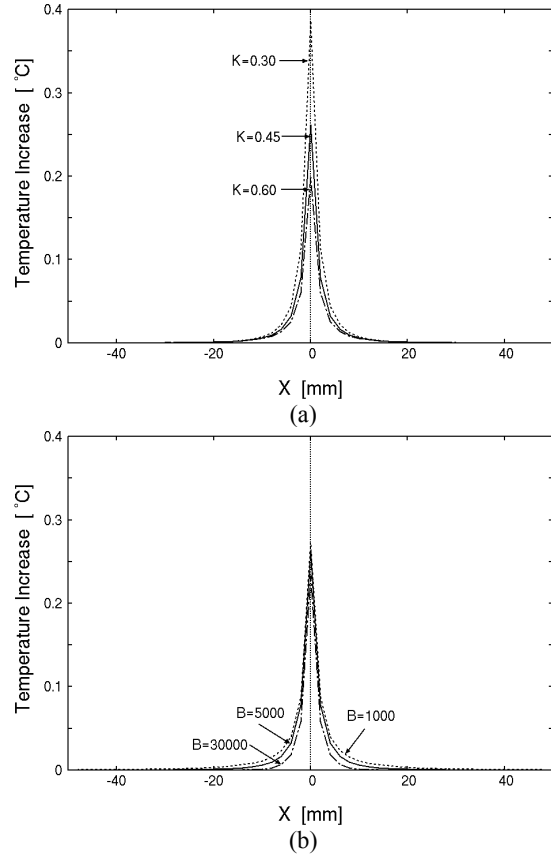

(a)

(b)

Fig.1 Green's function for a point heat source given at the center of the cube (the side length of 200 mm). Effect of (a) different heat conductivity and (b) different term associated with blood flow. $y=z=0$.

(a)

(b)
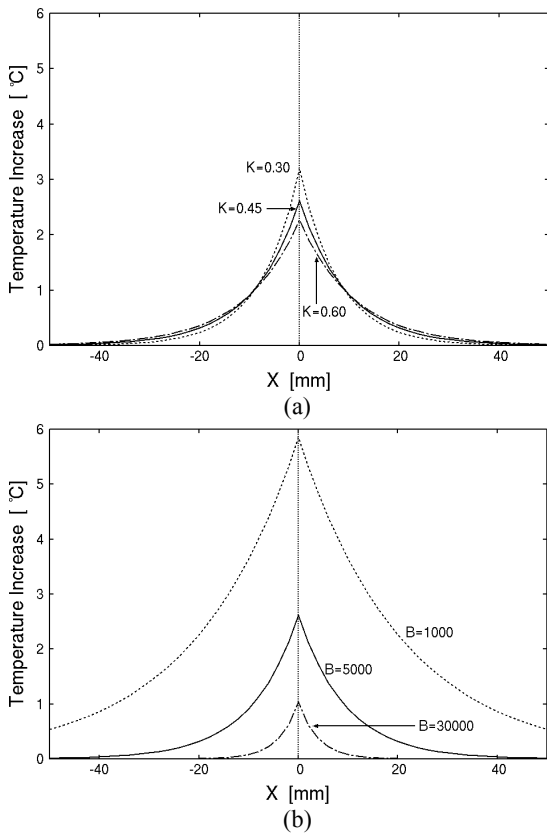
Fig.2. Green's function for plane heat source given at the *y-z* plane of the cube (the side length of 200 mm). Effect of (a) different heat conductivity and (b) different term associated with blood flow. *y=z*=0.

(a)

(b)

Fig. 3. Maximum temperature elevation divided by peak (a) 1-g and (b) 10-g average SARs for 1-D model.

application of heat source. Green's function indicates the thermal diffusion length under the application of a point heat source with unit strength, which roughly provides the volume where heat can diffuse. It is noteworthy that we investigated 1-D Green's function for a modified bioheat equation in [10]. For obtaining Green's functions, the FD method is used for simplicity, as is used for solving conventional bioheat equation. The cell size is set to 2 mm. Thermal diffusion length is defined as the length where the amplitude of heat decreases to (1/*e*). However, in this paper, this is defined as the length where the amplitude decreases to 5%, since the value is comparable to the FD cell length. For proper estimation of each effect on Green's function, one of the heat conductivity or blood flow rate is changed with the other parameter fixed. A point heat source with 1mW is given at the center cell of the cube with its side length of 200 mm. Figs. 1 (a) and (b) illustrate the effect of heat conductivity and blood flow rate on Green's function, respectively (*y=z*=0). The origin of the coordinate corresponds to the centre cell of the cube. The term associated with blood flow is fixed to 5000 W/m$^3 \cdot ^\circ$C in Fig. 1 (a) and the heat conductivity is set to 0.45 W/m·$^\circ$C in Fig. 1(b). From Fig. Fig. 1(a), the amplitude of
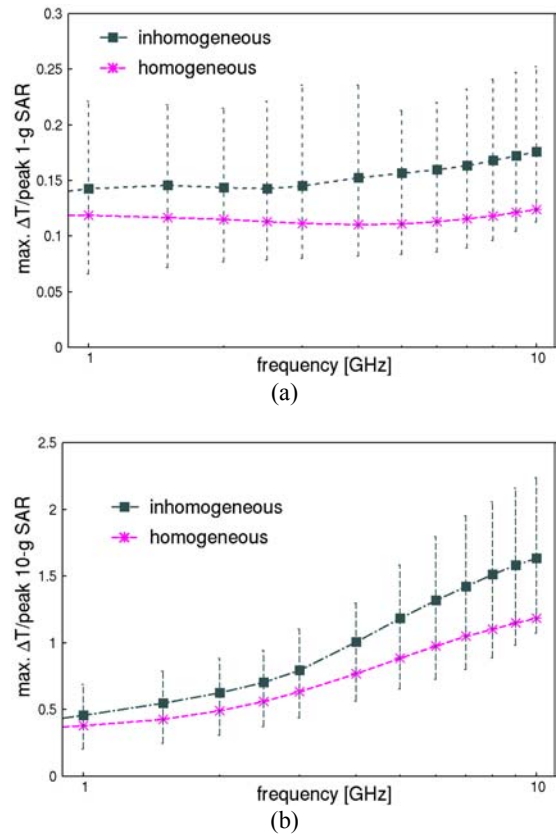
Green's function is affected by the heat conductivity by a factor of two. However, the thermal diffusion length is marginally affected by the heat conductivity: 6.55 mm for 0.30 W/m·$^\circ$C, 7.05 mm for 0.45 W/m·$^\circ$C, and 7.41 mm for 0.60 W/m·$^\circ$C. From Fig. 1(b), the thermal diffusion length is largely dependent on the blood flow rate: 8.91 mm for 1000 W/m$^3 \cdot ^\circ$C, 7.06 mm for 5,000 W/m$^3 \cdot ^\circ$C, and 5.19 mm for 30,000 W/m$^3 \cdot ^\circ$C. It should be noted that the peak amplitude at the heat source or the origin is almost independent on the blood flow.

In order to further investigate fundamental characteristics of heat diffusion in human tissues, heat sources are given on the *y-z* plane uniformly (*x*=0 mm), almost corresponding to a 1-D case. As seen from Fig. 2, the blood perfusion of human tissues is more dominant than that of heat conductivity for the temperature increase in a 1-D heat source, unlike for the case of a point source. This can be interpreted from Eq. (7), which states that the temperature increase is given by the superposition of green's function multiplied by heat potential (ρSAR).

Let us discuss the temperature increase due to RF near-field exposure, which is our main interest. The above Green's function suggested that the most dominant factor was the distance where heat can diffuse in a 3-D case. Main tissues

around the surface of the human head are skin, fat, muscle, glands, when excluding the pinnae. The term associated with the blood flow B is in the range of 1,000 and 10,000 $W/m^3 \cdot {}^\circ C$ (See Table II). Then, roughly speaking, a distance where heat can diffuse is up to 2-6 cm as seen from Fig. 2. The EM waves decrease exponentially from the surface of human tissue. For muscle, the penetration depth of EM waves is around 12 mm at 2 GHz. As can be seen from Eq. (7), SAR distribution and the Green's function determine the temperature increase. This implies that the volume or mass required for properly estimating maximum temperature increase is dependent on the frequency of the EM waves, i.e., no best mass exists for correlating the SAR and temperature increase over the whole frequency band considered in this paper. Namely, an appropriate average volume would become smaller at higher frequencies.

Figure 3 shows the frequency dependency of the ratio of maximum temperature increase to peak SAR averaged over 1g (a) and 10g (b) tissues for the one-dimensional model. The error bars for inhomogeneous model represent uncertainty caused by tissue composition. Since we consider the one-dimensional model, peak 1g and 10g SARs are defined as the SAR averaged over 10 mm and 22 mm thicknesses. As seen from this figure, the correlation between peak SAR and maximum temperature increase is dependent on the frequency. Comparing Figs. 3 (a) and (b), the correlation for the averaging mass of 1g is less sensitive to the frequency than that for the mass of 10g. The reason for this difference can be explained as follows. With the increase in the frequency, EM power absorption concentrates around the surface of the model, which is attributed to the increase of tissue conductivity. Now the averaging thickness is fixed, peak 10-g SAR increases moderately with the increase of the frequency. Maximum temperature increase also becomes large in accordance with the increase of peak SAR. Note that maximum temperature increase is not proportional to peak SAR, which is caused by heat conduction. The balance of increases between peak SAR and maximum temperature increase determines the frequency characteristics of the temperature increase and SAR.

Next, the effect of finite dimensions of an antenna is discussed using a cubic model, whose side length is 200 mm. Frequency dependency of the ratio of maximum temperature increase to peak SAR averaged over 1g and 10g tissues for cubic model is presented in Fig. 4. The curves for the one-dimensional model are also plotted in this figure for comparison. The values for the cubic model are smaller than those of 1-D model. The decrease of the maximum temperature increase divided by peak SAR becomes obvious at high frequencies. Additionally, the difference between 1-D and 3-D results is significant for the averaging mass of 10g. This is attributed to the finite dimension of the antenna. Namely, the contribution of SAR outside the averaging volume to maximum temperature increase is small at higher frequencies. Due to the balance between the effect of the penetration depth and antenna dimension, the maximum temperature increase divided by peak SAR for 10-g mass is
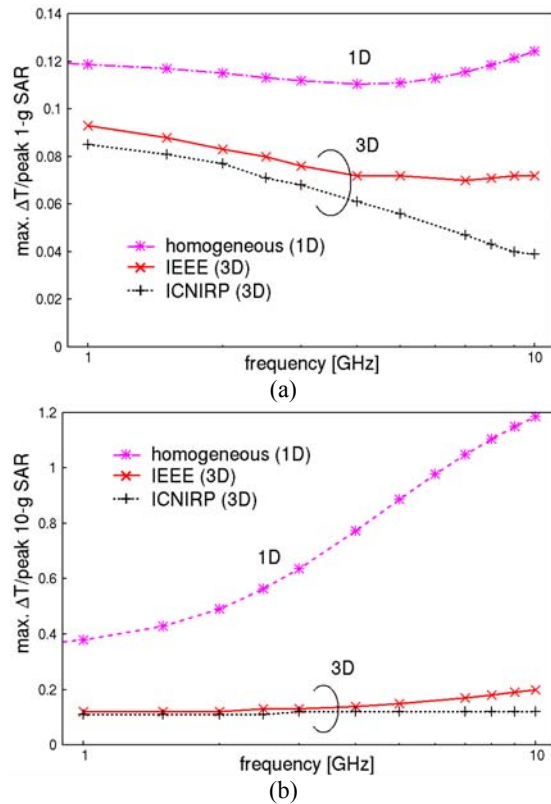

(a)

(b)

Fig.4. Maximum temperature elevation divided by peak (a) 1-g and (b) 10-g average SAR for a cubic model.
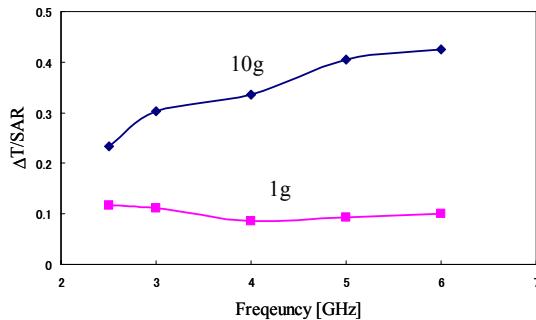

Fig.5. Maximum temperature elevation divided by peak SAR in an anatomically-based model.

less dependent on the frequency than for 1-g mass.

In order to confirm the findings using simplified models, we conducted calculations using an anatomically-based head models. Unlike the cubic model, pinnae exist in the anatomically-based model. In this discussion, SAR is averaged over the tissues in the head only (excluding the pinnae) following to the algorithm prescribed in IEEE. Maximum temperature increase in the head only was considered. As seen from Fig.5, better correlation was for

averaging mass of 1g than that of 10g, unlike those obtained suing the cubic model. This discrepancy could be attributed to the existence of the pinna where much energy is deposited, while we pay no attention to temperature increase in this organ.

4. Summary

This paper presented the correlation between peak spatial-average SAR and maximum temperature increase in the head models in the frequency band of 1-10 GHz. The effects of antenna size and frequency on the correlation were investigated separately. For explaining the effect of 3-D results, Green's function was introduced. For confirming the findings obtained in the simplified models, computations using an anatomically-based model were conducted. However, some discrepancy was observed in the results between cubic and anatomically-based models.

In future work, the effect of pinnae on this correlation will be discussed.

References

[1] J. Wang and O. Fujiwara, "FDTD computation of temperature rise in the human head for portable telephones," IEEE Trans. Microwave Theory & Tech., vol.47, pp.1528-1534, 1999.

[2] P. Bernardi, M. Cavagnaro, S. Pisa, and E. Piuzzi, "Specific absorption rate and temperature increases in the head of a cellular-phone user," IEEE Trans. Microwave Theory & Tech., vol.48, pp.1118-1126, 2000.

[3] P. Gandhi, Q.-X. Li, and G. Kang, "Temperature rise for the human head for cellular telephones and for peak SARs prescribed in safety guidelines," IEEE Trans. Microwave Theory & Tech., vol.49, no.9, pp.1607-1613, 2001.

[4] A. Hirata and T. Shiozawa, "Correlation of maximum temperature increase and peak SAR in the human head due to handset antennas," IEEE Trans. Trans. Microwave Theory & Tech., vol.51, pp.1834-1841, 2003.

[5] A. Dross, V. Santomaa, N. Kuster, "The dependence of electromagnetic energy absorption upon human head tissue composition in the frequency range of 300-3000 MHz," IEEE Trans. Microwave Theory & Tech., vol.48, pp.1988-1995, 2003.

[6] International Commission on Non-Ionizing Radiation Protection (ICNIRP), "Guidelines for limiting exposure to time-varying electric, magnetic and electromagnetic fields (up to 300 GHz)," Health Phys., vol.74, pp.494-522, 1998.

[7] IEEE C95.3-20902 Standard, 2002 (Annex E).

[8] J. Wang and O. Fujiwara, "Dosimetric evaluation of human head for portable telephones," Electron. & Comm. Japan, Part I, 2002.

[9] H. H. Pennes, "Analysis of tissue and arterial blood temperature in resting forearm," J. Appl. Physiol, vol.1, pp.93-122, 1948.

[10] Z.-S. Deng and J. Liu, "Analytical study on bioheat transfer problems with spatial or transient heating on skin surface or inside biological bodies," Trans. ASME J. Biomecha. Eng., vol.124, pp.638-649, 2002.

[11] A. Hirata, O. Fujiwara, T. Shiozawa, "Correlation between peak spatial-average SAR and temperature increase due to antennas attached to human trunk," IEEE Trans. Biomed. Eng., Aug. 2006 (in press).